Minimizing Equipment and Energy Cost in Mixed 10G and 100G/200G Filterless Horseshoe Networks with Hierarchical OTN Boards

Memedhe Ibrahimi[1*], Omran Ayoub[1], Aryanaz Attarpour[1], Francesco Musumeci[1], Andrea Castoldi[2], Mario Ragni[2] and Massimo Tornatore[1]

[1]Politecnico di Milano, Milano, 20133, Italy.
[2]SM-Optics, Vimercate MB, 20871, Italy.

*Corresponding author: memedhe.ibrahimi@polimi.it;

Abstract

Emerging 5G services are changing the way operators manage and optimize their optical metro networks, and the transmission technology and network design process must be tailored to the specific conditions in this segment of the network. Ensuring cost-efficient and energy-efficient network design requires novel approaches that optimize across all network layers. Therefore, to moderate the growth of operators' expenses, in this paper, we investigate low-cost and energy-efficient cross-layer deployment of hierarchical Optical Transport Network (OTN) boards minimizing equipment and energy consumption cost in mixed 10G and 100G/200G filterless metro networks. We propose an Integer Linear Programming (ILP) model and a Genetic Algorithm (GA) approach that decide: *i)* the node structure by deploying various stacked OTN boards (performing traffic-grooming at the electrical layer) and *ii)* lightpath establishment considering coherent and non-coherent transmission technologies. Simulative results on real filterless horseshoe networks with real traffic matrices show that our proposed approaches achieve up to 50% cost savings compared to real-world benchmark deployments.

Keywords: Cross-layer design, Traffic-grooming, OTN, coherent and non-coherent transmission

1 Introduction

The recent acceleration in fiber-to-the-home and new 5G deployments are pressuring operators to enhance their metro-aggregation network segment and to seek novel strategies to reduce equipment cost in this segment. To reduce network cost, optimizing the deployment of traffic-grooming boards and interfaces deployed in Optical Transport Network (OTN) equipment is crucial. However, accounting for a hierarchy of different OTN grooming boards while employing mixed coherent and non-coherent transmission technologies makes the problem extremely complex, as it accounts for the inter-dependency between the deployment of various types of OTN boards and the establishment of lightpaths at different rates (see Section 4 for more details).

In this paper, we devise a novel approach for low-cost deployment of OTN grooming boards with the aim of minimizing overall equipment and energy consumption cost. Specifically, we optimize the deployment of a hierarchical structure of various OTN boards and interfaces. The practical need to solve this problem comes from the fact that real-world metro and access deployments still employ legacy 10G technology [1], hence a gradual upgrade that mixes coherent (100G/200G) and non-coherent (10G) transmission technologies is required for cost-efficient short/mid-term network planning. Additionally, we solve the problem considering real filterless horseshoe networks, that currently represent a prominent candidate for cost-effective optical-network deployment and are characterized by optical-switching nodes equipped with passive optical power splitters/combiners instead of costly wavelength selective switches [2, 3, 4, 5]. To solve this problem, we provide an Integer Linear Program (ILP) model for the cross-layer joint deployment of OTN boards (performing traffic-grooming at electrical layer) and lightpath establishment at optical layer, while considering the wavelength broadcast nature of filterless networks, i.e., wavelength propagation beyond lightpath termination [6].

Note that the traffic-grooming problem to minimize the number of Add-Drop Multiplexers (ADMs) in SDH/SONET metro ring networks has been extensively researched in the early 2000s [7, 8, 9, 11, 12]. However, recent advances in transmission technologies have brought the need to decommission the SDH layer and remove legacy SDH equipment and all related complexity and cost [13] and the problem that we are solving here is substantially different. In fact, to the best of our knowledge, no previous works have tackled the grooming problem considering: *i)* the hierarchical grooming-node structure consisting of various *stacked* OTN boards, *ii)* the *co-existence of coherent and non-coherent transmission technologies* (100G/200G and 10G lightpaths), and *iii)* filterless node architecture that adds significant complexity to the problem as it impacts wavelength allocation and lightpath establishment.

To make our system modeling practical and applicable on real network deployments, we consider several types of OTN boards and interfaces with different features such as cost, capacity, energy consumption and transmission technology, i.e., coherent and non-coherent. Additionally, we account for the deployment of Dispersion Compensation Modules (DCUs) and channel filters

(to be used only in those solutions involving deployment of 10G lightpaths), and we ensure dedicated path protection (*DPP*) of traffic requests. To solve the problem of minimizing OTN equipment-deployment and energy-consumption cost (referred for simplicity as *minOTN* in the rest of the paper), we develop an ILP model and, due to the complexity of the problem, we also devise a Genetic Algorithm (GA) to solve larger instances.

The paper is organized as follows: in Section 2, we introduce related work. In Section 3, we describe the problem of minimizing OTN equipment deployment and energy consumption cost in metro horseshoe networks, while in Section 4 we describe the proposed strategies to solve this problem. In Section 5, we describe case studies and provide numerical results, and in Section 6 we conclude our work and provide the main takeaways.

2 Related work

Traffic-grooming in optical networks is a well-investigated topic [14, 15], however, most works focus on traditional approaches of bundling traffic requests on established lightpaths without any consideration for cross-layer optimization of the equipment performing the traffic-grooming and transmission technologies. In the following we overview some relevant works on classical traffic-grooming in wavelength division multiplexing (WDM) ring networks.

In [7, 8, 9, 10], authors minimize the total cost of ADMs, and transceivers [10], in SONET/WDM rings. The proposed heuristics assume the deployment of pairs of ADMs at nodes that establish the lightpath. These works consider one type of ADM, single-rate traffic requests of 155.52 Mbps and single-rate lightpaths with 2.5 Gbps capacity. Compared to these works, the main difference of our work, that significantly increased problem complexity is that we consider various types of stacked OTN boards (ADMs for electronic processing of traffic). Moreover, we also consider lightpaths of different rates and transmission technologies, i.e., coherent and non-coherent.

Delving more into the methodologies used to solve the problem of minimizing the number of ADMs in SONET rings, an ILP and a simulated-annealing heuristic are proposed in [11] and approximation algorithms in [12]. Number of ADMs in [11] is determined by connection types: in case of single-hop, an ADM is placed at source and destination nodes, while, in case of multi-hop, a hub node is defined with as many ADMs as number of lightpaths. In [12], the route of traffic demands is given as input, and the number of ADMs is then decided based on grooming of traffic and established lightpaths. Similarly, network cost minimization through an approximation algorithm is presented in [16]. The cost model accounts for both ADMs and optical components (OADMs) by deploying ADMs at end nodes of a lightpath and an OADM at every intermediate node.

Besides cost, several works have investigated the role of traffic-grooming towards green optical networks and power-efficient traffic grooming [17, 18]. ILP models and heuristic approaches are proposed to model the network power

consumption by relating total power consumption of the network to the power consumption of individual lightpaths and thus deciding grooming of traffic requests. Note that compared to these works, we jointly minimize equipment and energy consumption cost (accounting for the equipment at electrical layer and optical layer) and implement cross-layer optimization approaches.

3 Minimizing Equipment and Energy Cost in Filterless Horseshoe Networks with Hierarchical OTN Boards

3.1 Problem statement

The problem of minimizing equipment and energy cost in filterless horseshoe networks with hierarchical OTN boards (*minOTN*) can be summarized as follows: **Given** a filterless horseshoe topology, a set of traffic requests between node pairs, a set of candidate OTN boards and interfaces to be placed at each node, **decide** jointly: *i)* the deployment of OTN boards and interfaces (including location and type), DCU modules and filters for non-coherent traffic, and *ii)* the route and wavelength assignment (RWA) and traffic-grooming of traffic requests, **constrained by** *i)* traffic-processing capacity of each OTN board and interface type, *ii)* maximum number of client interfaces given for each board, *iii)* wavelength capacity, *iv)* filterless networks constraints on wavelegth assignment and *v)* ensuring dedicated path protection for traffic requests, with the **objective** of minimizing equipment and energy consumption cost of deployed equipment (OTN boards and interfaces, transponders, DCU modules and filters).

3.2 Problem modeling

We consider three types of OTN boards (see Fig. 1.a): *OTU2-ADM*, *OTU4-ADM* and *OTU-TPD*. *OTU2-ADM* enables users to connect via access interfaces, performs traffic-grooming and establishes non-coherent 10G lightpaths via 10G colored interfaces, i.e., 10G transponders. *OTU4-ADM* enables users to connect via access interfaces, forwards traffic to/from *OTU2-ADM* and *OTU-TPD* and performs traffic-grooming; *OTU-TPD* forwards traffic to/from *OTU4-ADM* and establishes coherent 100G/200G lightpaths.

Fig. 1.a shows the node structure and highlights the interconnection of OTN boards and interfaces. Fig. 1.b shows interconnected filterless horseshoe topologies considered in our study and Fig. 1.c shows an illustrative example of traffic-grooming. In Fig. 1.a, a user (*src*) can either connect through 1G or 10G access interfaces (E_0) to *OTU2-ADM* (N_{1AP}) or *OTU4-ADM* (N_{2AP}). Traffic across boards is forwarded via line interfaces: E_4 and E_5. Additionally, coherent (100G/200G) lightpaths are established between ROADM and transponders (E_6) and non-coherent lightpaths (10G) are established between ROADM and 10G transponders (E_7).

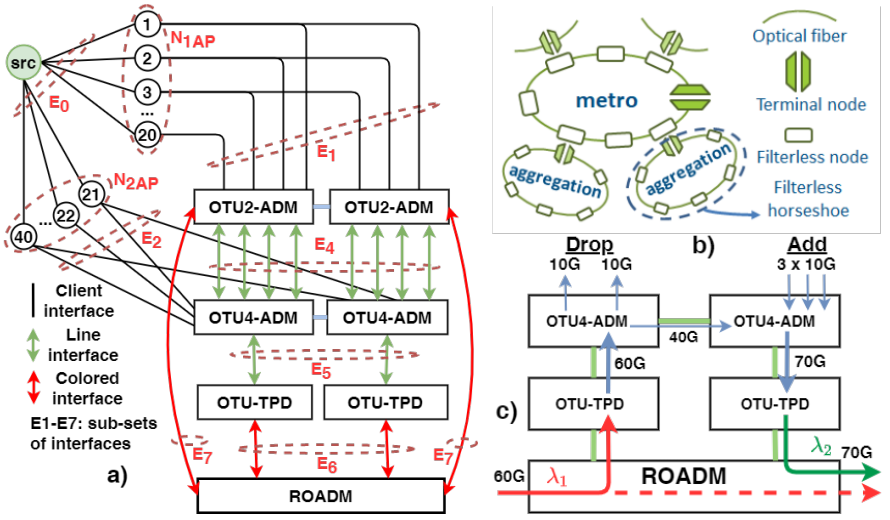

Fig. 1: a) Hierarchical node structure, showing boards and interfaces and connections between boards; b) interconnected filterless horseshoe topologies; c) illustrative example of traffic grooming

Board placement constraints. *OTU4-ADM* and *OTU-TPD* are deployed in pairs (east and west) and traffic can be carried from one side to the other for grooming with added traffic. *OTU2-ADM* placement is not constrained in pairs, as traffic can be forwarded directly to ROADM via 10G transponders. However, as we ensure dedicated path protection (*DPP*) at OTN board level, placement of board pairs may be constrained if traffic requests are to be protected. Traffic incoming to *OTU-TPD* is forwarded to *OTU4-ADM* and reaches its destination via *OTU4-ADM* or *OTU2-ADM* client interfaces, or it is forwarded to the *OTU4-ADM* pair and groomed with added traffic. Traffic incoming to ROADM can be forwarded to *OTU2-ADM* through 10G transponders to either be dropped or groomed with added traffic. Number of *OTU2-ADM* interfaces is set to eight (per direction) to match the number of ROADM ports. Each OTN board has a maximum number of clients, e.g., ten, that can connect to it (constraint on *E1* and *E2* for each board).

An illustrative example of traffic-grooming is shown in Fig. 1.c. A 100G lightpath (λ_1) carrying 60G traffic is dropped at *OTU-TPD* (west). Traffic is forwarded electrically to *OTU4-ADM* (blue arrow) and two 10G traffic requests are dropped at *OTU4-ADM* west (*Drop*) while the remaining 40G are carried over to *OTU4-ADM* east. The carried 40G traffic is groomed with the added three 10G traffic requests at *OTU4-ADM* east (*Add*) and a 100G lightpath carrying 70G traffic is established at *OTU-TPD* east (λ_2). As we consider filterless node architecture, λ_1 propagates beyond destination (dashed line) and cannot be re-used.

Table 1: Set and subsets

N	Set of logical nodes representing OTN boards and interfaces
N_1, N_2, N_3, N_4	Subset of logical nodes representing *OTU2-ADM*, *OTU4-ADM*, OTU-TPD boards and ROADMs
N_{1AP} N_{2AP}	Subset of logical nodes representing client interfaces of *OTU2-ADM* and *OTU4-ADM* boards
E	Set of links representing optical links and connection between interfaces of OTN boards
E_0	Subset of logical links representing connections of a client to interfaces of *OTU2-ADM* and *OTU4-ADM*
E_1, E_2	Subset of logical links representing connections to client interfaces to *OTU2-ADM*and *OTU4-ADM*, respectively
E_4	Subset of links representing the line interfaces between *OTU2-ADM* and *OTU4-ADM*
E_5	Subset of links representing the line interfaces between *OTU4-ADM* and *OTU-TPD*
E_6	Subset of links representing coherent colored interfaces between *OTU-TPD* and ROADM
E_7	Subset of links representing non-coherent colored interfaces between *OTU2-ADM* and ROADM
E_R	Subset of links representing links between ROADM nodes
D	Set of connection requests (demands)
W	Set of wavelengths

Table 2: Decision variables and parameters

$x_{i,j}^{s,t}$	Binary variable equal to 1 if demand (s,t) uses link (i,j)
$y_{i,j}$	Binary value equal to 1 if link (i,j) is activated/used
δ_j	Binary variable equal to 1 if logical node j, i.e., OTN board/interface, is used
$\tau_{i,w}$	Binary variable equal to 1 if transponder i is activated and uses wavelength w
$f_{i,j,w}$	Binary variable euqal to 1 if wavelength w is used in active link (i,j)
$z_{i,j}^{s,t,w}$	Binary variable equal to 1 if wavelength w is used on link (i,j) for demand (s,t)
λ_w	Binary variable equal to 1 if wavelength w is used in the network (in any link $f_{i,j,w}$)
$b_{i,j,w}$	Binary variable equal to 1 if wavelength w is being broadcasted on link (i,j)
$d_{i,j}$	Binary variable equal to 1 if a DCU module is placed in link (i,j)
$\Gamma_{i,j}$	Capacity of link (i,j)
μ_i	Cost of logical node i, i.e., OTN board/interface
$v_{s,t}$	Traffic in Gbps generated by demand (s,t)
Γ_w	Capacity of wavelength, 10G for non-coherent and 100G/200G for coherent
$\pi_{s,t}$	Parameter equal to 1 or 2, indicating if demand (s,t) is protected
ρ_{AP}	Parameter equal to 10, the maximum number of client interfaces of an OTN board
κ_{N1}	Parameter equal to 4, the maximum number of interfaces for each *OTU2-ADM*

4 Strategies to solve *minOTN*

To solve *minOTN* we have developed an ILP model (presented in Sec. 4.1) and, to scale with larger problem instances, we developed a Genetic Algorithm (GA) (described in Sec. 4.2). We benchmark our proposed approaches to a state-of-the-art approach, referred to as Omnibus (OB) (described in Sec. 4.3).

4.1 Integer Linear Programming

In this section we introduce the ILP model. The sets and decision variables are provided in Table 1 and Table 2, respectively. For a visual representation of sets and subsets, refer also to Fig. 1.a. The objective function minimizes cost of deployed equipment, i.e, OTN boards, interfaces, transponders, DCU modules and filters.

4.1.1 Objective function

The objective function is to minimize the cost (μ) of logical nodes (δ), i.e., OTN boards and interfaces, that are deployed and cost (μ) of transponders ($\tau_{i,w}$) used to establish lightpaths on wavelength w.

$$\min \sum_{j \in N} \delta_j * \mu_j + \sum_{i \in N_3, w \in W} \tau_{i,w} * \mu_i \tag{1}$$

4.1.2 Constraints

$$\sum_{(i,j) \in E} x_{i,j}^{s,t} - \sum_{(j,i) \in E} x_{j,i}^{s,t} = \begin{cases} \pi_{s,t}, & \text{if } i = s \\ -\pi_{s,t}, & \text{if } i = t \\ 0 & \text{otherwise} \end{cases} \qquad \forall i \in N, (s,t) \in D \tag{2}$$

Constraint (2) is the solenoidality constraint and ensures the flow conservation between source and destination nodes, and serves to ensure protection of traffic demands. Constraints (3) and (4) refer to the maximum number of client interfaces, e.g., ten, for each *OTU2-ADM* and *OTU4-ADM* board. Constraint (5) is the capacity constraint for each link *(i,j)*.

$$\sum_{(i,j) \in E_1} y_{i,j} \leq \rho_{AP} \quad \forall j \in N_1 \tag{3}$$

$$\sum_{(i,j) \in E_2} y_{i,j} \leq \rho_{AP} \quad \forall j \in N_2 \tag{4}$$

$$\sum_{(s,t) \in D} x_{i,j}^{s,t} * v_{s,t} \leq \Gamma_{i,j} \qquad \forall (i,j) \in E \tag{5}$$

Constraints (6)-(10) are consistency constraints. Eq. (6) implies that link *(i,j)* is activated only if there is a traffic demand *(s,t)* going through it, while Eq. (7) enforces that link *(i,j)* is not activated unless there is at least one demand passing through it. Eq. (8) and (9) ensure logical node *i*, i.e., OTN board or interface, is activated if logical link *(i,j)* is used, i.e., traffic is passing through node *i*. Eq. (10) ensures that traffic flowing in *(i,j)* direction can not return back in *(j,i)* direction.

$$x_{i,j}^{s,t} \leq y_{i,j} \qquad \forall (i,j) \in E \tag{6}$$

$$\sum_{(s,t) \in D} x_{i,j}^{s,t} \geq y_{i,j} \quad \forall (i,j) \in E \tag{7}$$

$$\delta_j \geq y_{i,j} \quad \forall j \in N, (i,j) \in E \tag{8}$$

$$\delta_i \geq y_{i,j} \quad \forall i \in N, (i,j) \in E \tag{9}$$

$$x_{i,j}^{s,t} + x_{j,i}^{s,t} \leq 1 \qquad \forall (i,j) \in E, (s,t) \in D \tag{10}$$

Constraints (11)-(16) disallows traffic to by-pass client interfaces. Eq. (11)-(13) enforce that client traffic is routed through one logical link of subset E_0 and either an *OTU2-ADM* (N_{1AP}) or *OTU4-ADM* (N_{2AP}) client interface is activated for routing demand *(s,t)*. Eq. (14)-(16) enforce that traffic reaching an interface is not by-passed through logical links E_0, E_1 or E_2.

$$\sum_{(i,j)\in E_0} \sum_{(s,t)\in D} x_{i,j}^{s,t} \leq 1 \qquad \forall j \in N_{1AP} \cup N_{2AP} \quad (11)$$

$$\sum_{(i,j)\in E_0} \sum_{(s,t)\in D} x_{i,j}^{s,t} \leq 1 \qquad \forall i \in N_{1AP} \cup N_{2AP} \quad (12)$$

$$\sum_{(s,t)\in D} x_{j,k}^{s,t} \leq 1 \qquad \forall (i,j) \in E_0 \quad (13)$$

$$x_{i,j}^{s,t} + x_{j,k}^{s,t} \leq 1 \qquad \forall (i,j) \in E_0, (j,k) \in E_0, (s,t) \in D \quad (14)$$

$$x_{i,j}^{s,t} + x_{j,k}^{s,t} \leq 1 \qquad \forall (i,j) \in E_1, (j,k) \in E_1, (s,t) \in D \quad (15)$$

$$x_{i,j}^{s,t} + x_{j,k}^{s,t} \leq 1 \qquad \forall (i,j) \in E_2, (j,k) \in E_2, (s,t) \in D \quad (16)$$

Colored interfaces/links. The following constraints refer to the colored links characterized by a wavelength *w*. Eq. (17) and (18) are consistency constraints ensuring $f_{i,j,w}$ is "*1*" if link *(i,j)* is activated and a demand *(s,t)* uses wavelength *w*. Eq. (19) and (20) are specific for ROADM nodes, i.e., $j \in N_4$, and Eq. (21) and (22) serve to impose that traffic incoming to the ROADM node either passes through an express link or it is dropped to a *OTU-TPD* or *OTU2-ADM*. Eq. (23) is a consistency constraint and Eq. (24) represents the wavelength capacity constraint.

$$f_{i,j,w} \leq y_{i,j} \qquad \forall w \in W, (i,j) \in E_6 \cup E_7 \cup E_R \quad (17)$$

$$z_{i,j,w}^{s,t} \leq f_{i,j,w} \qquad \forall w \in W, (i,j) \in E_6 \cup E_7 \cup E_R, (s,t) \in D \quad (18)$$

$$z_{i,j,w}^{s,t} = z_{j,k,w}^{s,t} \qquad \forall j \in N_4, w \in W, (s,t) \in D \quad (19)$$

$$\sum_{(i,j)\in E_R} x_{i,j}^{s,t} + \sum_{(j,k)\in E_R} x_{j,k}^{s,t} \leq 1 \qquad \forall j \in N_4, (s,t) \in D \quad (20)$$

$$\sum_{(i,j)\in E_6\cup E_7} f_{i,j,w} \leq 1 \qquad \forall j \in N_4, w \in W \quad (21)$$

$$\sum_{(j,k)\in E_6\cup E_7} f_{j,k,w} \leq 1 \qquad \forall j \in N_4, w \in W \quad (22)$$

$$\sum_{w\in W} z_{i,j,w}^{s,t} = x_{i,j}^{s,t} \qquad \forall (i,j) \in E_6 \cup E_7 \cup E_R, (s,t) \in D \quad (23)$$

$$\sum_{(s,t)\in D} z_{i,j,w}^{s,t} \leq \Gamma_w \qquad \forall (i,j) \in E_6 \cup E_R \cup E_7, w \in W \quad (24)$$

Constraints (25)-(28) refer to *OTU2-ADM* interfaces. Each *OTU2-ADM* board can have at most four active interfaces, colored for 10G transponders, line interfaces connecting to *OTU4-ADM* or a combination of the two.

$$\sum_{(j,i)\in E_4\cup E_7} y_{j,i} \leq \kappa_{N1} \quad \forall j \in N_1 \quad (25) \qquad \sum_{(i,j)\in E_4\cup E_7} y_{i,j} \leq \kappa_{N1} \quad \forall j \in N_1 \quad (26)$$

$$y_{j,i} = y_{i,j} \qquad \forall (i,j) \in E_4 \quad (27) \qquad y_{j,i} = y_{i,j} \qquad \forall (i,j) \in E_7 \quad (28)$$

Eq. (29) and (30) refer to DCU module placement: if variable $f_{i,j,w}$ is active and wavelength w on link *(i,j)* is 10G, a DCU module is placed per direction.

$$d_{i,j} \leq f_{i,j,w} \qquad \forall (i,j) \in E_R, w \in W \quad (29) \qquad d_{i,j} \geq f_{i,j,w} \quad \forall (i,j) \in E_R, w \in W \quad (30)$$

Constraints (31) and (32) refer to coherent transponder deployment (light-path establishment). If colored link $f_{i,j,w}$ is active then a transponder at wavelength w is placed at *OTU-TPD* board. $\tau_{i,w}$ is a binary variable equal to 1 if a transponder is deployed at the interface of *OTU-TPD* i on wavelength w.

$$M * \tau_{i,w} \geq f_{i,j,w} + f_{j,i,w} \qquad \forall i \in N_3, (i,j) \in E_6, w \in W \quad (31)$$

$$\sum_{w\in W} \tau_{i,w} \leq 1 \qquad \forall i \in N_3 \quad (32)$$

Constraints (33)-(36) are the filterless constraints. Eq. (33) and (34) imply that if a wavelength w is used in a link *(i,j)* then λ_w is set to "1". If $\lambda_w = 1$, then all the colored links *(i,j)*, i.e., $f_{i,j,w}$ are equal to "1" for w, implying that wavelength w can not be re-used. Eq. (35) and (36) enforce that if wavelength w is broadcasted on link *(i,j)* then $b_{i,j,w}$ is equal to 1.

$$M * \lambda_w \geq \sum_{(i,j)\in E_R} f_{i,j,w} \qquad \forall w \in W \quad (33) \qquad \sum_{(i,j)\in E_7\cup E_6} f_{i,j,w} \leq 1 \quad \forall w \in W \quad (34)$$

$$b_{i,j,w} \leq \lambda_w * y_{i,j} - f_{i,j,w} \qquad \forall (i,j) \in E_R, w \in W \quad (35)$$

$$b_{i,j,w} \geq \lambda_w * y_{i,j} - f_{i,j,w} \qquad \forall (i,j) \in E_R, w \in W \quad (36)$$

Note that, the high complexity of the problem leads to scalability issues for the ILP as even relatively small network instances, e.g., 5-node and 6-node topologies, have millions of variables. The number of variables of the ILP model is equal to: $((1+W)(2E+ED+N+1)-1)$ and the number of constraints is equal to: $(E_6+E_7+E_R)(2W+DW+D)+D(E_0^2+E_1^2+E_2^2+N+N_4+3N_4W+1)+2W(1+2E_R)+N_3(1+WE_6)+3N_1+N_2+2N_{1AP}+2N_{2AP}+5E+E_0+E_4+E_7$. To cope with the scalability issues of the complete ILP model, we adopt a Lexicographic optimization approach [20], however, we do not elaborate in detail for the sake of brevity.

4.2 Genetic Algorithm

Given a physical network topology and a set of traffic requests, GA decides the structure of the nodes, i.e., OTN boards/interfaces and their interconnection, performs lightpath establishment and decides the grooming of traffic requests. We developed a GA approach to solve the *minOTN* problem since GA is a suitable approach for solving complex placement problems [19]. Solving *minOTN* is done in two steps: *i)* initialization and *ii) GA for OTN board placement.*

The *initialization* phase generates the list of all candidate paths to route demands between source-destination node pairs, i.e., accounting for all possible combinations of lightpath establishment and the corresponding OTN boards and interfaces needed to route the demand.

GA for OTN board placement makes use of candidate paths generated during *initialization* and explores the combinations of OTN board placement and lightpath establishment that ensure a feasible solution and minimizes the equipment and energy cost of the network.

4.2.1 Initialization

To generate candidate paths, we present each node through a logical representation consisting of seven nodes, as shown in Fig. 2. A connection request outgoing/ingoing form/to a node can be routed either through 10G interfaces of *OTU2-ADM* or TPD. As traffic may be routed on the left or right side of a horseshoe, we logically consider left ROADM and right ROADM for each node. The top node connects to 10G interfaces and TPD, and accounts for the internal node structure, i.e., interconnection of OTN boards and interfaces.

An illustrative example of how the candidate paths for a connection request between node-1 (*N1*) and node-2 (*N2*) are generated is given in Fig. 2. The figure shows four candidate paths: traffic is routed through 10G colored interface and a non-coherent lightpath is established between *N1* and *N2* (red dashed line), or it is routed through TPDs and a coherent lightpath is established between *N1* and *N2* (green dashed line). Alternatively, a lightpath is established between *N1*s left TPD and *N2*s right TPD (yellow dashed line). As we consider all possible paths, we account for cases when traffic is groomed

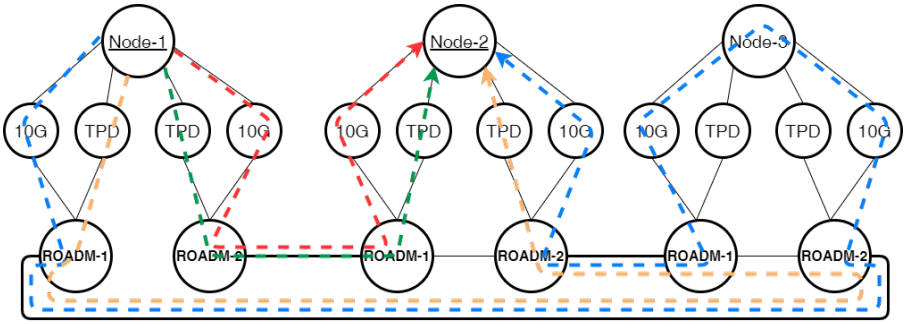

Fig. 2: Illustrative example of a three node topology and a subset of candidate paths for a connection request between Node-1 and Node-2

with other requests and goes through boards of another node but it is not dropped. For example, traffic is routed through *N1*s left 10G colored interface in a lightpath between *N1* and *N3*. Traffic is passed through *N3*s right 10G interface to *N3*s left 10G interface (across *OTU2-ADM* boards), and a new lightpath is established between *N3* and *N2* to carry traffic to its destination. In this case, it is necessary to establish two lightpaths and use two wavelengths (imposed by filterless node constraints: wavelength re-use is not possible). Note that for the sake of simplicity, we are not showing all possible paths between *N1* and *N2*.

4.2.2 GA for board placement

We model *minOTN* as an evolutionary process driven by competition among members (solutions) of the population. Fig. 3 shows a high-level structure of main building blocks of the GA. An initial population is generated, and fitness and feasibility of members of the population are calculated. GA operators such as selection, crossover and mutation are performed on members of the population and then the next generation is created. GA stops when the stopping condition is met.

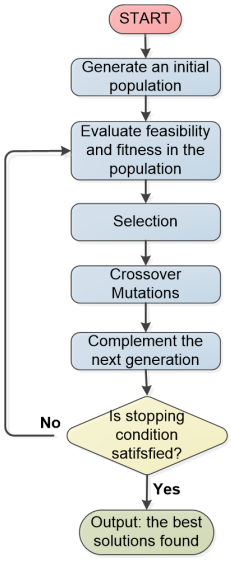

Fig. 3: A general structure of the GA

We encode OTN board/interface placement and routing of demands through gene clusters and genes: we consider a gene cluster for each demand and, in each gene cluster, we consider as many genes as there are candidate paths to route the demand. Fig. 4 shows an example of three gene clusters, each representing a demand and the corresponding n genes, each representing a candidate path. A gene cluster with an active *gene 1* implies the demand is routed along the path encoded by *gene 1* and accounts OTN board and interface placement necessary to route the connection.

A GA solution represents a placement of OTN boards, interfaces, transponders, routing of demands and the established lightpaths with wavelength

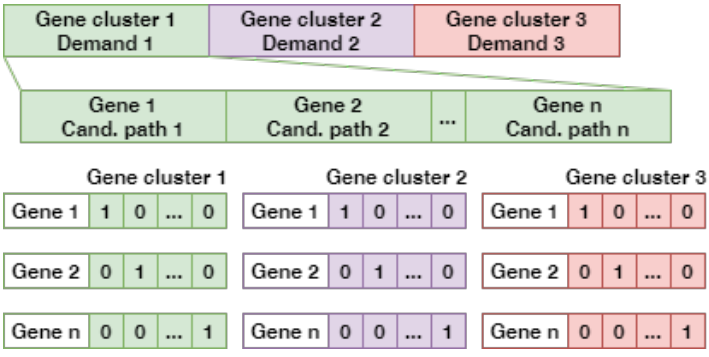

Fig. 4: Illustrative example of three gene clusters and the corresponding genes representing candidate paths

assignment. Each solution is characterized by its *fitness value* and *feasibility* that indicate how good is a GA solution. *Fitness value* refers to total cost of deployed equipment (we minimize cost, so a lower *fitness value* is desirable). *Feasibility* refers to constraints violation: a solution has feasibility equal to one, if it satisfies all constraints of the problem.

A set of GA solutions represents a population. The initial population is generated at random and new populations are generated according to *tournament selection policies* that define the pairs of solutions to participate in the tournament. Once the GA starts finding feasible solutions, members of the population are sorted in three groups: *A)* feasible solutions with a *low* fitness value, *B)* feasible solutions with a *high* fitness value and *C)* unfeasible solutions with a 95% feasibility. We consider a solution to have a *low* (*high*) fitness value if it is not 0.5% (5%) higher than the best solution found so far. Solutions from group *A* participate in the tournament 70% of the time, solutions from group *B*, 20%, and solutions from group *C*, 10% of the time. *Tournament rules* are defined as follows: *i)* a feasible solution wins over an unfeasible solution; *ii)* if two feasible solutions compete, the solution with the lower fitness wins and *iii)* if two unfeasible solutions compete, the winner is chosen at random. New generations are created by performing genetic operations (crossover - parts of the solutions are exchanged between two solutions; and mutation - genes are randomly selected and inverted) on tournament winners.

The GA searches for the best solution until the *stopping condition* is met. The stopping condition can be defined according to a fixed number of generations or according to some rule. We set the GA stopping condition as a fixed number of generations, e.g., five thousand. If there is no improvement in the objective function for fifty generations, we consider GA to be in a *stuck* state (GA reaches a local optimum). In this case, all feasible solutions which have a *low* fitness value are deleted to restart the search process and escape the local minimum - we refer to this as *hecatomb*. Once the *stopping condition* has been met, the GA outputs the best solution found.

4.3 Benchmark approach: Omnibus (OB)

In the OB benchmark approach, board placement is performed considering that 100G lightpaths are established between all neighboring nodes, hence traffic-grooming is performed at every node. Specifically, *OTU4-ADM*s are deployed at each node to perform traffic-grooming at the electrical layer. In case traffic cannot be served by an OB with single 100G lightpaths, an upgrade is adopted at nodes generating/handling more traffic by doubling the deployed equipment. We consider OB as a benchmark scenario as it represents the state-of-art approach for real-world OTN boards deployment. An illustrative example of Omnibus deployment is shown in Fig. 5 for a three node topology. A 100G coherent lightpath is established between each neighbor node pair and traffic is groomed at *OTU4-ADM* boards. Colored arrows represent traffic destined to each corresponding node (purple to N1, orange to N2, blue to N3), groomed traffic (at the electrical layer) and the 100G lightpaths. Note that,

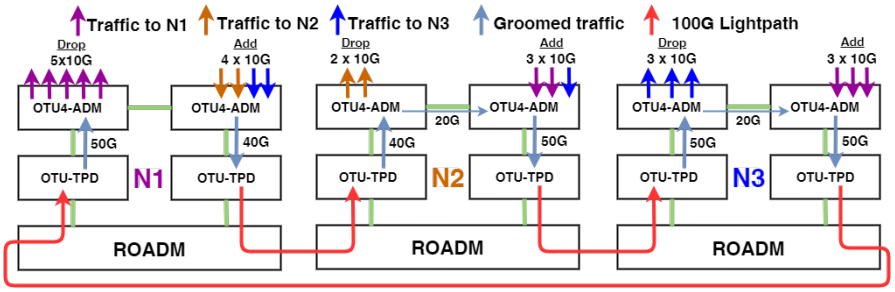

Fig. 5: Illustrative example of Omnibus implementation in a three node topology. Traffic requests: 2 x 10G N1→N2 (orange), 2 x 10G N1→N3 (blue), 1 x 10G N2→N3 (blue), 2 x 10G N2→N1 (purple), 3 x 10G N3→N1 (purple)

traffic requests shown serve for illustrative purposes only and do not imply actual generated traffic between nodes.

5 Illustrative numerical results and discussion

This section presents numerical results. We first provide the evaluation settings and the cost and energy models (see Sec. 5.1 and Sec. 5.2). Then, we compare the performance of ILP, GA and OB on real filterless horseshoes in terms of equipment cost (see Sec. 5.3), and total equipment and energy consumption cost (see Sec. 5.4).

5.1 Evaluation settings

For our experimental evaluations, we consider real filterless horseshoe topologies (see Fig. 1.b) of 5-nodes and 6-nodes with three traffic matrices. We implemented the ILP using AMPL and CPLEX 12.10 solver, and the GA was developed in *C++* programming language. All evaluations for ILP and GA are performed on a workstation with Intel(R)Cor(TM) i7-6700K CPU (4.00GHz × 8) and 32 GB of memory.

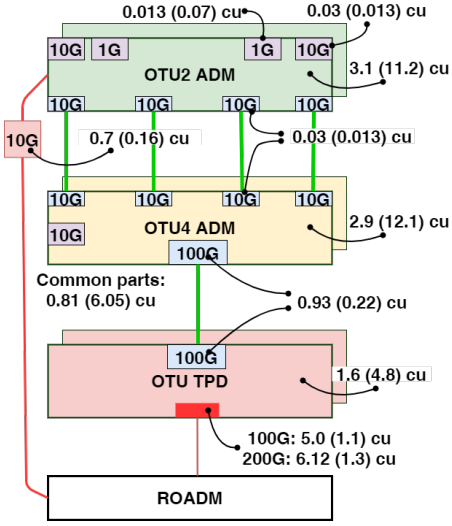

Fig. 6: Cost of equipment and in brackets electricity cost for a year, in cost units (*cu*)

We consider three traffic matrices (TM): *i)* TM1: real-world traffic matrix with unprotected 10G traffic request and protected 1G traffic requests. Traffic requests are bi-directional and amount to a total of 224 Gbps for 5-node horseshoe and 316 Gbps for 6-node horseshoe; *ii)* TM2: TM1 + 45% additional unprotected 10G traffic

requests; and *iii)* TM3: TM1 + 60% additional protected and unprotected 10G traffic requests. Due to a non-disclosure agreement with our industry partner, we can not provide more detailed information about traffic matrices.

5.2 Cost and energy models

Fig. 6 reports equipment cost and in brackets, the energy consumption cost for one year, in cost units (cu).

Cost model. The cost of equipment ($Equipment_{cost}$), i.e., OTN boards and interfaces, is given in Fig. 6. Additionally, if a 10G lightpath is established, we deploy a DCU module (0.53 cu) on each link (one per direction), a filter (0.37 cu) for each $OTU2\text{-}ADM$ and a channel filter (0.43 cu) at the receiver for each established 10G lightpath. We consider a *common parts* cost representing the cost of a shelf where OTN boards are placed: a shelf can host at most a pair of same type OTN boards and in case more boards are deployed, cost is added accordingly. Equipment cost is provided by our industry partner and values are arbitrarily altered to preserve a confidential disclosure agreement.

Energy consumption model. Given the normalized power consumption values from our industry partner, we calculate the electricity cost for a year for each deployed equipment ($Electricity_{cost}$). From [5], we adopt average power consumption of 120 watts (W) for a 100 Gbit/s PM-QPSK transponder and price of electricity estimated to be 0.001 cu/kWh. We scale according to the normalized power consumption values provided by our industry partner and calculate the cost of electricity for a year in cu. Fig. 6 shows the equipment cost and in brackets electricity cost for a year in cost units (cu). The analysis is then performed over an N number of years, described in detail in Sec. 5.4. Considering both equipment and energy cost in the objective function implies that cost for each equipment is given as:

$$Total_{cost} = Equipment_{cost} + N * Electricity_{cost} \tag{37}$$

5.3 Equipment cost minimization

Fig. 7 shows the total cost (and its breakdown) of deployed equipment in terms of equipment type for the 5-node (Fig. 7(a)) and 6-node topologies (Fig. 7(b)), for TM1, TM2 and TM3 considering ILP, GA and OB deployment strategies. Note that for the 6-nodes topology, only the results for GA and OB are reported, as the ILP fails to find a solution even after a week of running time. As the figure contains a lot of information, let us divide its description in three phases.

First, let us start by validating the performance of GA comparing its performance to that of the ILP model. Fig. 7.a shows that ILP and GA reach the same equipment cost in case of TM1 and TM2, while in case of TM3, GA reaches a 4% higher equipment cost compared to ILP. In terms of execution time, GA finds a solution in under 5 minutes while ILP takes up to 9 hours. This validates GA performance and we can conclude that GA reasonably approximates ILP performance, while reaching a solution in less time.

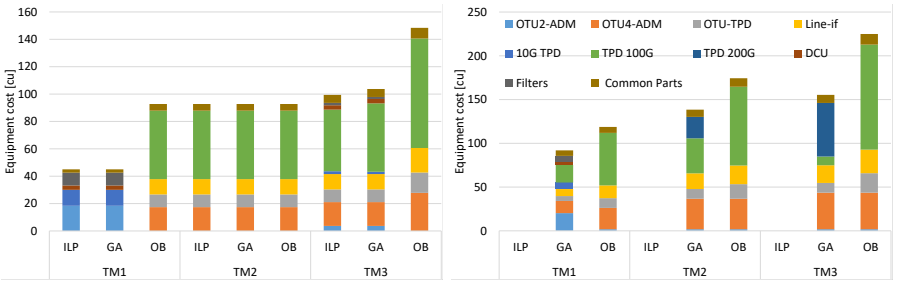

Fig. 7: Total equipment cost and cost contribution of each equipment of equipment in case of ILP, GA and OB deployment for a) 5-node horseshoe and b) 6-node horseshoe topologies

Second, let us compare the cost minimization achieved by our proposed ILP and GA with the OB baseline solution, and explore the value of each cost contribution in the breakdown. Fig. 7.a shows that, in comparison to OB, ILP and GA achieve cost savings of 51% and 30% in case of TM1 and TM3, respectively. The optimized deployment by GA and ILP allows significant cost savings due to a predominant deployment of 10G transponders instead of coherent 100G transponders as in OB. Regarding TM1, in case of ILP and GA, *OTU2-ADM* compose 41% of cost, 10G transponders compose 26% while filters, DCU modules and *common parts* compose 21%, 7% and 5%, respectively. In case of OB, 100G transponders (*TPD 100G*) and *OTU-TPD* compose 64% of cost, *OTU4-ADM* 19%, line interfaces 12% and *common parts* 5%. In case of TM2, ILP and GA reach the same solution as OB. The reason is that in case of TM1, 100G lightpaths are populated around 50%, so there is sufficient residual capacity to serve the added traffic for TM2 without additional equipment. We observe that TM2 traffic is distributed such that the most cost-effective solution is establishing 100G lightpaths that are just sufficient to serve traffic requests. Moreover, results in case of TM2 show that OB, for some specific values of offered traffic, provides a practical and cost-efficient benchmark approach. In case of TM3, ILP and GA employ mixed coherent and non-coherent technologies. In particular, 100G transponders (*TPD 100G*) and *OTU-TPD* compose 56% of cost while equipment employing non-coherent 10G lighpaths, i.e., *OTU2-ADM* with 10G transponders (*10G TPD*), filters and DCU modules, compose 12% of total cost. Cost savings are achieved due to the use of 10G transponders instead of over-provisioning with additional 100G coherent transponders as in OB.

Third, let us focus on the results obtained on the 6-node network. Fig. 7.b shows that GA cost savings compared to OB vary between 21% and 31%. On average, cost savings are lower compared to 5-node topology as we do not observe a case of non-coherent 10G lightpaths only as in case of 5-node TM1, leading to highest cost savings. Actually, we observe that in case of 6-node TM1, the cost contribution is distributed among 10G and 100G transponders and the corresponding OTN equipment, i.e., *OTU2-ADM* and *OTU4-ADM* boards. In case of TM2 and TM3, compared to 5-node topology,

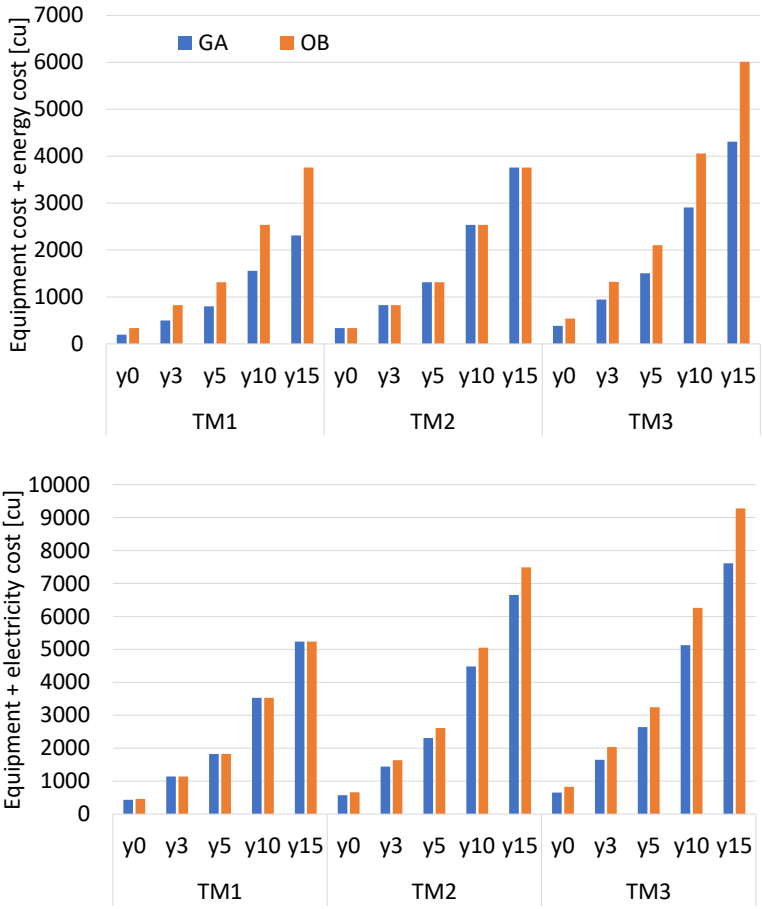

Fig. 8: Equipment + electricity cost in cost units (*cu*) for a) 5-node horseshoe and b) 6-node horseshoe in case of TM1, TM2 and TM3 for GA and OB

GA employs only coherent lightpaths and besides 100G transponders, deploys 200G transponders as well. In fact, 33% and 86% of deployed transponders are 200G transponders (*TPD 200G*), in case of TM2 and TM3, respectively. The reason GA deploys 200G transponders is due to a higher traffic and that it is more cost-efficient to deploy one 200G transponder instead of two 100G transponders as in case of OB.

5.4 Equipment and energy cost minimization

Due to the importance of energy cost, especially when considering the entire network lifetime, in this subsection we perform a further analysis considering the total network cost expressed as the sum of equipment and energy cost.

We compare the network cost achieved by GA and OB, for both the 5-nodes and 6-nodes horseshoe topologies, considering TM1, TM2 and TM3.

For each TM[1], we consider a different network lifetime (and hence different energy consumption cost, i.e., electricity cost) over $N = 0$, 3, 5, 10 and 15 years (note that 0 years means that energy cost is zero, N years means that we account for the energy cost along N years). For each topology we report: *i)* total equipment and electricity cost, to observe overall cost increase over N years (see Fig. 8) and *ii)* equipment cost (when equipment and electricity cost are jointly minimized), to observe if node structure, i.e., deployment of OTN boards, changes when accounting for energy costs (see Fig. 9).

First, we observe the total cost of equipment and electricity for TM1, TM2 and TM3 over a period of 15 years (*y0* up to *y15*). Fig. 8.a and Fig. 8.b show a linear increase in total cost due to increase of electricity consumption over the years for 5-node horseshoe and 6-node horseshoe, respectively. Fig. 8.a shows that GA achieves cost savings between 28% and 42% in case of TM1 and TM3 compared to OB. In case of TM2, the cost of GA is equal to OB due to same equipment deployment. In case of 6-node horseshoe, Fig. 8.b shows that in case of TM1, GA achieves 6% cost savings up to *y3*, while after *y3* the total cost is the same as OB (detailed discussion on why this happens is given in the next paragraphs). In case of TM2 and TM3, GA achieves cost savings between 11% and 19% compared to OB.

Second, we observe equipment cost when equipment and electricity cost are jointly minimized over N years (note that focusing only on equipment cost allows us to verify if, by accounting electricity cost, the actual equipment deployment changes with respect to results shown in previous subsection). Fig. 9.a shows that in case of 5-node topology, for all the three traffic matrices, the equipment cost does not change, whichever network lifetime is considered. In other words, the solution in terms of equipment deployment is always the same, independently of how long is the network lifetime (and hence the energy cost) that we are considering, hence cost breakdown contribution matches the analysis in Sec. 5.3. In the figure, we report only *y0* and *y3* since deployment between *y3* and *y15* remains the same. Note that, we do not claim that this result holds true for all equipment vendors, as they may have different energy consumption values. Nonetheless, based on real-world cost model and energy consumption model considered here (provided by our industry partner), electricity cost of equipment tends to be proportional to the equipment cost and, therefore, regardless of whether equipment cost is minimized only or if the electricity cost is included, the node structure (in terms of choice of OTN boards) does not change.

To stress the fact that the previous result is not necessarily generalizable, in Fig. 9.b we repeat the same experiment on a 6-node horseshoe. We observe that, for example, in case of TM1, total equipment cost is lower for N less than three (92 *cu* vs 120 *cu*). In fact, in case $N < 3$, mixed transmission technologies (coherent and non-coherent) are deployed, implying deployment of both *OTU2-ADM* and *OTU4-ADM* boards. Instead, in case $N \geq 3$, coherent

[1]Note that each of three TMs is kept constant along the years in our experiments, as we assume that the network is deployed in the aggregation segment of the metro network, where traffic is stable over time.

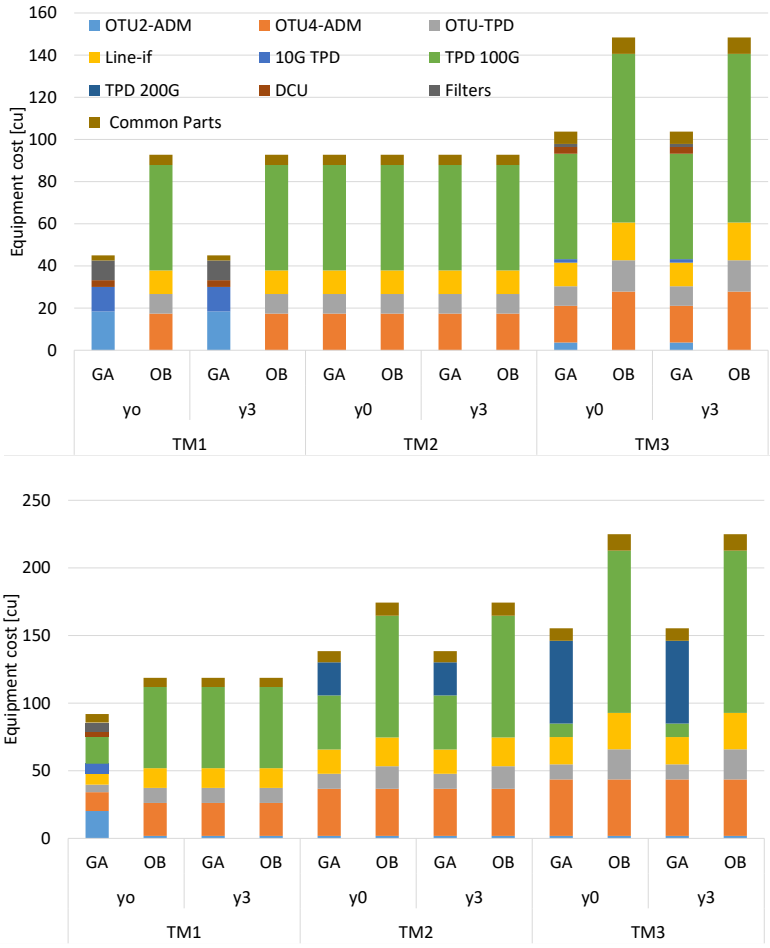

Fig. 9: Equipment cost in cost units (*cu*) for a) 5-node horseshoe and b) 6-node horseshoe in case of TM1, TM2 and TM3 for GA and OB

transmission technologies are deployed, e.g., 100G lightpaths (*TPD 100G*), and hence only *OTU4-ADM* boards. The reason deployment changes after three years is mostly attributed to the cost of *common part*, i.e., shelf for hosting boards. Given that shelf electricity cost is significantly higher than shelf equipment cost (6.05 *cu* vs 0.81 *cu*), when planning for three or more years, it is more convenient to place same board types, i.e., *OTU4-ADM*, instead of a combination of board types, i.e., *OTU2-ADM* and *OTU4-ADM*. This is because when deploying both types of OTN boards, two shelves are needed to host the boards. Additionally, as N increases, the impact of electricity cost becomes more decisive. In Fig. 9 we report cost values for *y0* and *y3* only since deployment for $N \geq 3$ remains the same.

Observing equipment cost contribution (breakdown) in case of $N < 3$, we notice that equipment deployed to establish non-coherent 10G lightpaths, i.e.,

OTU2-ADM boards, 10G transponders, DCU modules and filters, accounts for 41% of total cost while equipment deployed to establish coherent 100G lightpaths, i.e., *OTU4-ADM* and *OTU-TPD* boards, line interfaces and 100G transponders, accounts for 52% of total cost. The remaining 6% cost contribution is due to *common parts*. Conversely, in case of $N \geq 3$, cost contribution pertains only to equipment deployed to establish coherent 100G lightpaths.

Moving our attention to TM2 and TM3, Fig. 9.b shows again the joint minimization of equipment cost and electricity cost leads to same node structure deployment over the years. This implies that planning at *y0* ensures lowest-cost equipment deployed for the next N years. Consequently, cost breakdown contribution matches the analysis in Sec. 5.3.

In conclusion, 6-node TM1 is a particular case study in which network planning over N years leads to different equipment deployments, when accounting for energy cost. Therefore, care must be taken when energy cost is minimized along with equipment cost as depending on the case study it might lead to different lowest-cost equipment deployment.

6 Conclusion

In this paper, we investigated the problem of low-cost deployment of OTN traffic-grooming boards with the aim of minimizing equipment cost and energy consumption cost. We considered a hierarchical grooming-node structure consisting of various stacked OTN boards and the co-existence of coherent and non-coherent transmission technologies (100G/200G and 10G lightpaths). To solve this problem we proposed two optimization approaches, an integer linear programming (ILP) model and a genetic algorithm (GA), and compared their performance with a real-world benchmark deployment in real filterless horseshoe networks. The main takeaways and messages of the paper, can be summarized as the following:

- The GA and ILP ensure up to 50% savings in equipment cost compared to benchmark OB. Additionally, the performance of GA is validated and meets the optimality of ILP in significanly less time.
- The co-existence of coherent and non-coherent transmission technologies proves to be cost-efficient compared to benchmark OB that implies only deployment of coherent transmission technologies. Moreover, a mixed coherent and non-coherent transmission technology deployment is in line with a gradual update of currently deployed metro networks that still employ legacy 10G technology.
- Jointly minimizing equipment cost and energy consumption cost allows us to plan for over N years and ensures a low-cost equipment deployment that is proofed to be the minimal-cost network design for up to $N = 15$ years.
- Our proposed GA approach ensures low-cost network design when energy consumption cost is jointly minimized with equipment cost and achieves overall cost savings of up to 42% compared to OB.

The current version of *minOTN* can be further extended to account for further real-life deployment constraints. Therefore, as a future work, we plan to account for the specific physical layer non-linearities raising when mixing 10G/100G/200G lightpaths, as these non-linearities are particularly intense when mixing intensity-modulated transmission (as in 10G transmission) and coherent transmission(as in 100G/200G interfaces).

Acknowledgment

The work leading to these results has been supported by a sponsored research agreement with SM-Optics. We thank in particular our colleagues Giorgio Parladori and Rosanna Pastorelli.

Conflicts of interest

Not applicable.

References

[1] E. Virgillito, *et al.*, "Experimental Validation of QoT Computation in Mixed 10G/100G Networks." ACP Conference, 2021.

[2] O. Karandin, *et al.*, A techno-economic comparison of filterless and wavelength-switched optical metro networks," in International Conference of Transparent Optical Networks, (2020), pp. 1–4.

[3] P. Pavon-Marino, *et al.*, "Techno-Economic Impact of Filterless Data Plane and Agile Control Plane in the 5G Optical Metro," in Journal of Lightwave Technology, vol. 38, no. 15, pp. 3801-3814, 2020.

[4] F. Paolucci, *et al.*, "Disaggregated edge-enabled C+L-band filterless metro networks," in Journal of Optical Communications and Networking, vol. 12, no. 3, pp. 2-12, 2020.

[5] O. Ayoub, , *et al.*, "Tutorial on filterless optical networks [Invited]," in Journal of Optical Communications and Networking, vol. 14, no. 3, pp. 1-15, 2022.

[6] C. Tremblay, *et al.*, "Filterless optical networks: a unique and novel passive WAN network solution," in IEICE Proceedings Series, vol. 49, 2007.

[7] O. Gerstel, *et al.*, "Wavelength assignment in a WDM ring to minimize cost of embedded SONET rings," in *IEEE INFOCOM* 1998.

[8] A. L. Chiu and E. H. Modiano, "Traffic grooming algorithms for reducing electronic multiplexing costs in WDM ring networks," in *IEEE/OSA JLT*, vol. 18, no. 1, pp. 2-12, 2000.

[9] O. Gerstel, *et al.*, "Cost effective traffic grooming in WDM rings," in *IEEE INFOCOM*, 1998.

[10] O. Gerstel, *et al.*, "Cost effective traffic grooming in WDM rings," in *IEEE/ACM Transactions on Networking*, vol. 8, no. 5, pp. 618-630, 2000.

[11] J. Wang, *et al.*, "Improved Approaches for Cost-effective Traffic Grooming in WDM Ring Networks: Nonuniform Traffic and Bidirectional Ring," in *IEEE/OSA JLT*, vol. 19, no. 11, pp. 1645-1653, 2001.

[12] L. Epstein, *et al.*, "Minimization of SONET ADMs in ring networks revisited," in *Computing*, vol. 87, no. 1, pp. 3-19, 2010.

[13] SM-Optics, "Network Modernization: SDH bye-bye," whitepaper, 2018. *https://www.sm-optics.com/index.php/catalogs?download=5:smo-micro-otn-in-network-modernization*

[14] R. Dutta, *et al.*, "Traffic grooming for optical networks: foundations, techniques and frontiers," in *Springer Science & Business Media*, 2008.

[15] B. Mukherjee, I. Tomkos, M. Tornatore, P. Winzer, and Y. Zhao, "Springer Handbook of Optical Networks," in *Springer Nature*, 2020.

[16] M. Flammini, *et al.*, "The Traffic Grooming Problem in Optical Networks with Respect to ADMs and OADMs: Complexity and Approximation," in *Algorithms*, vol. 14, no. 5, pp. 1-12, 2021.

[17] S. Huang, D. Seshadri and R. Dutta, "Traffic Grooming: A Changing Role in Green Optical Networks," in *GLOBECOM*, 2009.

[18] E. Yetginer and G. N. Rouskas, "Power Efficient Traffic Grooming in Optical WDM Networks," in *GLOBECOM*, 2009.

[19] M. Ibrahimi et al., "QoT-Aware Optical Amplifier Placement in Filterless Metro Networks," in IEEE Communications Letters, vol. 25, no. 3, pp. 931-935, 2021.

[20] M. Ehrgott, " Multicriteria optimization," in Springer Science & Business Media, vol. 491, 2005.